Cooperative Research and Development Agreement (CRADA) Final Report

Report Date:

12/15/2024

In accordance with Requirements set forth in the terms of the CRADA, this document is the CRADA Final Report, including a list of Subject Inventions. It is to be forwarded to the DOE Office of Scientific and Technical Information upon completion or termination of the CRADA, as part of the commitment to the public to demonstrate results of federally funded research.

Parties to the Agreement: General Atomics & Berkeley Lab

CRADA number: FP13683

CRADA Title: Performance Testing of Low-resistance Demountable HTS Joints for Large Segmented Magnets

Responsible Technical Contact at Berkeley Lab: Reed Teyber / Xiaorong Wang

Name and Email Address of POC at Partner Company(ies):

Nikolai Norausky, Nikolai.Norausky@ga.com

Sponsoring DOE Program Office(s):

Office of Fusion Energy Sciences

LBNL Report Number:

LBNL-2001634

OSTI Number:

[SPO to complete]

Joint Work Statement Funding Table showing DOE funding commitment:

DOE Funding to LBNL	$259,070
Participant Funding to LBNL	n/a
Participant In-Kind Contribution Value	$155,000
Total of all Contributions	$155,000

Provide a list of publications, conference papers, or other public releases of results, developed under this CRADA:

(Publications must include journal name, volume, issue, Digital Object Identifier)

n/a.

Provide a detailed list of all subject inventions, to include patent applications, copyrights, and trademarks:

(Patents and patent applications are to include the title and inventor(s) names. When copyright is asserted, the Government license should be included on the cover page of the Final Report)

n/a

Executive Summary of CRADA Work:

In collaboration with the team at General Atomics, we measured the electrical resistance between the terminations of high-temperature superconducting cables in a background magnetic field at 4.2 K, liquid-helium boiling temperature. The termination concept we evaluated can be a critical component for the superconducting magnet system in a future fusion power plant. The measured electrical resistance value of the termination concept can provide important technical guidelines for engineers developing the superconducting magnet system for future fusion devices that can generate clean electricity for society.

Summary of Research Results:

The program objectives are to characterize the background field performance of CORC® demountable joint samples. The CORC® demountable joint samples were designed and fabricated by GA, and then sent to LBNL for self-field and background field performance characterization. A 77K performance testing campaign was conducted and novel PCB Hall probe arrays were developed to improve the joint testing diagnostics. The background field performance characterization required the completion of the LBNL hybrid test facility, where two high current magnet powering and synchronized protection systems are operated concurrently. The main deliverable of the program is a successful test of the demountable joint resistance as a function of background magnetic fields up to 6 Tesla in the bore of CCT 5. We conclude with a discussion of the diagnostic data during the test, unresolved questions which arose during the program, and recommendations for future work. Figure 1 *highlights the measured joint resistance as s function of background magnetic fields at 4.2 K, the main results of the work. More details of the results from the work can be found in a separate and dedicated report prepared by Dr. Reed Teyber.*

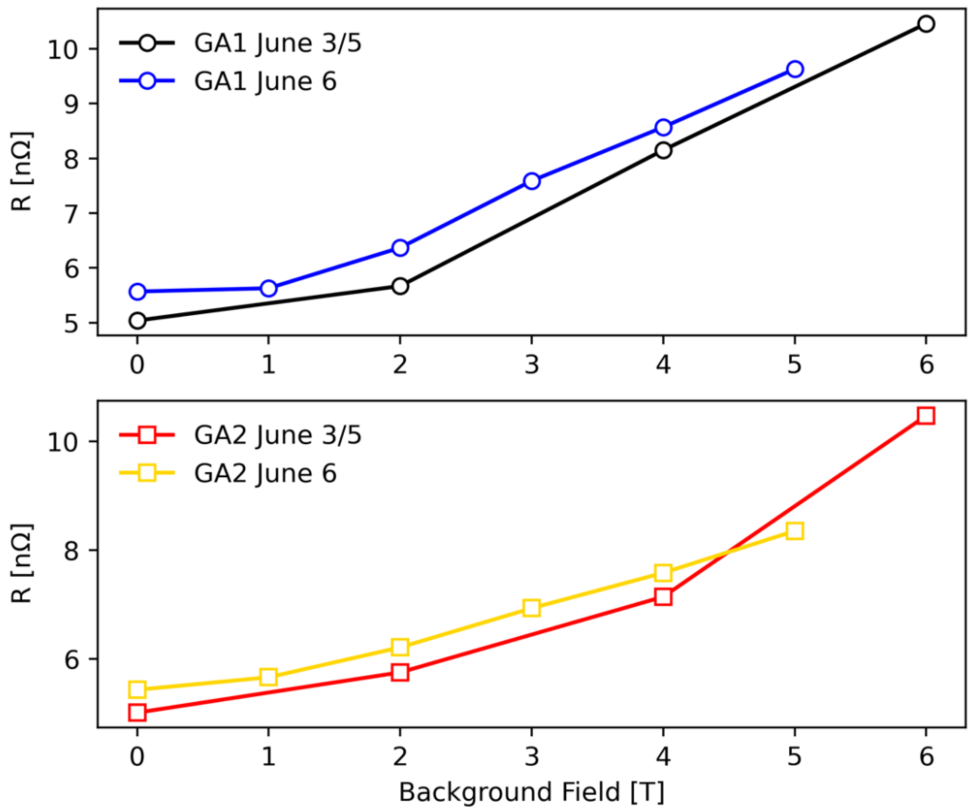

Figure 1 Joint resistance as function of background magnetic fields at 4.2 K.

We performed all the tasks listed in the original scope of work. We prepared the test setup by developing dedicated sample holders and completed the terminations to connect the sample to the test facility. We developed and measured mock-up joint samples and verified the measurement protocol for superconducting joint samples at room temperature and 77 K. We tested the superconducting CORC® joint samples in self-field at 77 and 4.2 K. We also tested superconducting CORC® joint samples in background fields at 4.2 K. Throughout the work, we exchanged with collaborators at GA and updated the status of the work.

Our work strengthened the collaboration between LBNL and General Atomics on the high-temperature superconducting magnet technology. The results from the work validate the technical feasibility of the demountable joint technology developed by General Atomics.

Performance Testing of Low-Resistance Demountable HTS Joints for Large Segmented Magnets

Prepared by Reed Teyber for General Atomics on behalf of the Lawrence Berkeley National Laboratory team

rteyber@lbl.gov

Table of Contents

1.0 Introduction *6*

2.0 Initial Performance Analysis *6*

2.1 PCB Hall Probe Array 13

3.0 Bolt Force and Contact Pressure Investigation *14*

4.0 Insert Probe and Facility Preparations *22*

5.0 Background Field Performance Characterization of CORC Demountable Joints *27*

6.0 Unresolved and Driving Questions *32*

4.0 Conclusion *33*

References *33*

1.0 Introduction

ReBCO cables are an enabling technology for compact fusion reactors, due to the high critical temperature and high critical field. These High Temperature Superconducting (HTS) cables have the potential to enable demountable superconducting fusion magnets that would allow easier access for machine maintenance. To realize this, demountable HTS joints are required with practical fabrication and assembly procedures, low resistances and uniform performance for current injection and extraction into the individual tapes. Ref. [1] and the references therein outline present state-of-the-art as applied to the CORC cable geometry produced by Advanced Conductor Technologies LLC (ACT).

This report outlines a Department of Energy (DOE) office of Fusion Energy Sciences (FES) INFUSE program on CORC Demountable joints as a collaboration between General Atomics (GA) and Lawrence Berkeley National Laboratory (LBNL). The program objectives are to characterize the background field performance of CORC demountable joint samples. The CORC demountable joint samples were designed and fabricated by GA, and then sent to LBNL for self-field and background field performance characterization. A 77K performance testing campaign was conducted and novel PCB Hall probe arrays [2] were developed to improve the joint testing diagnostics. The background field performance characterization required the completion of the LBNL hybrid test facility, where two high current magnet powering and synchronized protection systems are operated concurrently. The main deliverable of the program is a successful test of the demountable joint resistance as a function of background magnetic fields up to 6 Tesla in the bore of CCT 5 [3]. The report concludes with a discussion of the diagnostic data during the test, unresolved questions which arose during the program, and recommendations for future work.

2.0 Initial Performance Analysis

The demountable samples and clamping structure were prepared by General Atomics and sent to LBNL. The LBNL testing focused on samples “12-4-5.3 (2)” and “12-4-5.3 (4)”. The first step at LBNL was to solder the termination of the free end of the CORC cable to enable the first 77K performance measurements as shown in Figure 1. The length of the CORC cable protruding from the demountable joint samples was not long enough to follow the standard ACT soldering procedure; the tapes were forced to be constrained as shown in the bottom of Figure 1 (layers were not un-furled into termination). This is believed to result in slightly elevated upstream tape termination resistances. Although the focus of this program is to measure the resistance of the demountable joint, the upstream resistances impact the current distribution in the cables, which may contribute to the some of the phenomena observed and discussed later in this report.

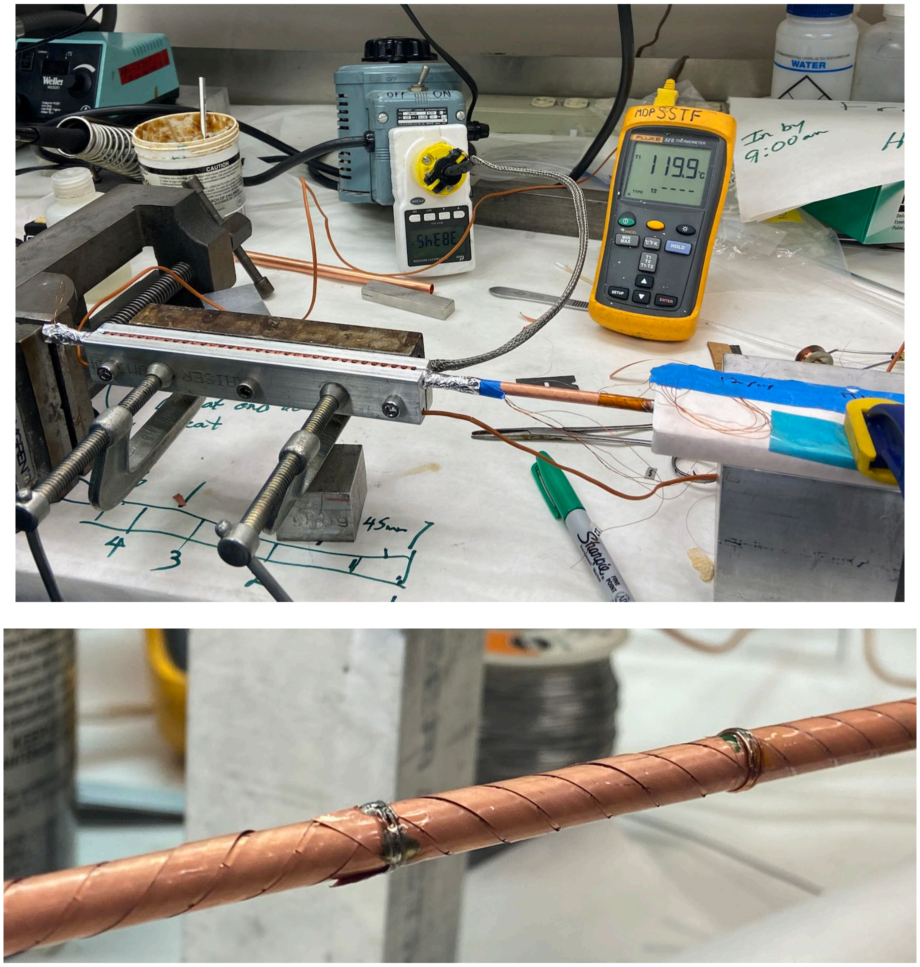

Figure 2: Indium soldering of demountable joint, showing flute-style joint (Top). Fixing layers to enable joint on short-length cable (Bottom).

The soldered samples were then prepared for the first iteration of 77K testing as shown below in Figure 2. The approximate voltage tap locations and their names are shown in the bottom of the figure. The two voltage taps "GA1" and "GA2" measure the demountable joint performance and will be referred to commonly throughout this report. These voltage taps include the bare copper-to-copper demountable interface resistance, the resistance of the bulk copper, and an unknown portion of the termination resistance (i.e. from ReBCO tape through solder to copper termination), as the exact location of voltage taps in a standard CORC terminations is not perfectly defined in all standard CORC terminations. Several NI-9238 measurement cards (four channel, 24 bit, 50 kHz simultaneous) were purchased for the project and used throughout the program for the joint characterization.

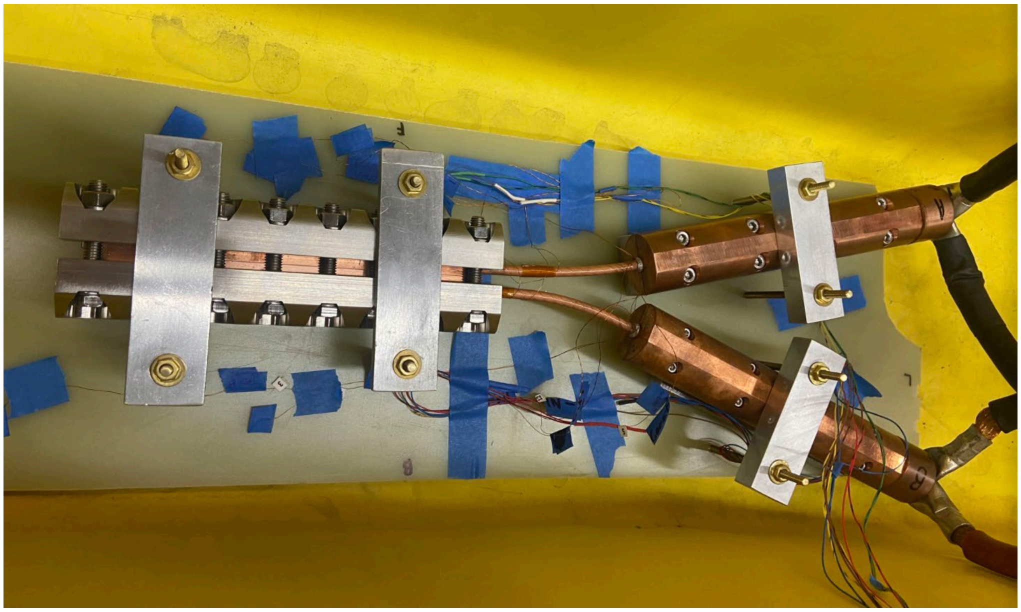

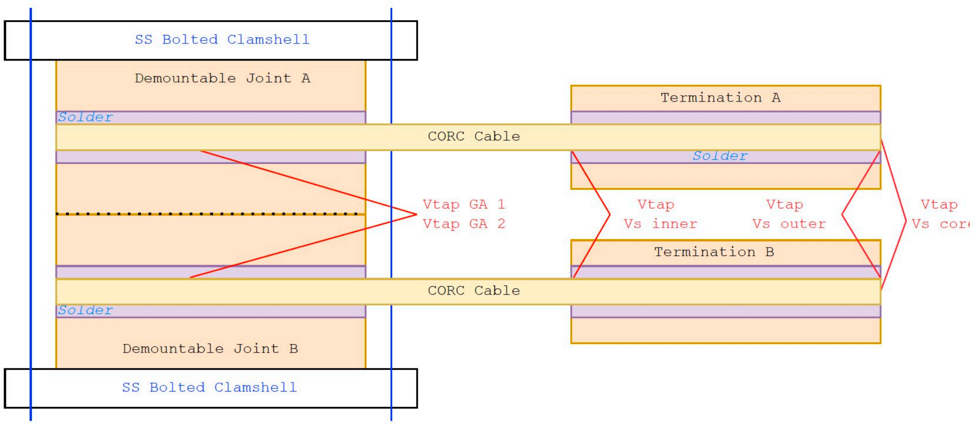

Figure 3: GA demountable joint mounted on G10 sheet for initial 77 K testing (top). Voltage tap naming and approximate locations (bottom).

The first set of testing is described below and shown in Figure 5 and Figure 6. Figure 5 shows the V-I measurements of voltage taps GA1 (top), GA2 (middle) and Vs Outer (bottom). Voltage taps GA1 and GA2 are the demountable joint resistance, and Vs Outer consists of the total upstream cable voltage as shown in Figure 2. The resistance in the legend is evaluated between 0-200A, and Figure 6 shows the same data as Figure 5 however with the linear region removed to highlight the nonlinearity in the joint resistance in these measurements. The caption shows the joint assembly (A1, A2, A3) and the thermal cycle within that joint assembly (TC1,…). The testing sequence with notes are summarized below.

Assembly 1 (A1)

- *Thermal Cycle (TC) 1-3*
    - Virgin prepared sample. The bolts were torqued to 25 ft-lb and there were no Belleville washers. On the third thermal cycle, there was a substantial increase in joint resistance on GA1 only (from ~48 to 220 nOhm in GA1). It is surprising that voltage tap GA 2 did not have a similar increase in joint resistance.
- *Thermal Cycle (TC) 4*
    - Bolts re-torqued to 25 ft-lb without disassembling joint. This more-or-less restored the contact resistance.
- *Thermal Cycle (TC) 5, 6, and 7*
    - Belleville washers installed without disassembling joint, which resulted in elevated joint resistance (from ~40 nOhm to ~75 nOhm in GA1). A more detailed investigation of Belleville washers is presented later in this report.
- *Thermal Cycle (TC) 8*
    - Belleville washers removed and re-torqued bolts to 25 ft-lb. The joint performance significantly reduced to ~ 230 nOhm in GA1.

After assembly 1 thermal 8, the sample was fully disassembled, revealing surface corrosion on the interface as shown in Figure 3. The corrosion pattern here (two bands along outer edges on top and bottom of photo) loosely follow the contact pressure distribution, which is presented in more detail later in this report. Note that the interface was never exposed. The interface was re-cleaned and the joint was reassembled with 25 ft-lb of torque before testing assembly 2.

Figure 4: Surface oxidation observed on demountable joint interface between assembly 1 and assembly 2, even though sample was clean when assembled and never disassembled between thermal cycles.

Assembly 2 (A2)

- *Thermal Cycle (TC) 9*

  Virgin powering for this reassembly. Although the joint resistances are much lower than the A1 TC5-9, they are higher than A1 TC1,2 and 4. Comparing the two virgin tests A1 T1 and A2 T9, the GA1 joint resistance increased to 48 nOhm from 37 nOhm.
- *Thermal Cycle (TC) 10*

  Thermal cycle after a full warmup-cooldown.

The sample was fully disassembled and re-cleaned thoroughly before reassembly into assembly 3, as shown in Figure 4.

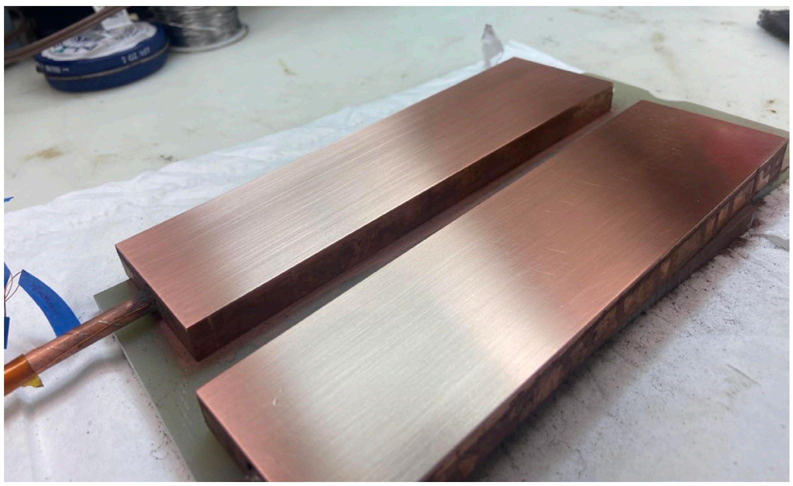

Figure 5:Re-cleaned interface after preparation right before clamping into assembly 3.

Assembly 3 (A3)

- *Thermal Cycle (TC) 1*
  - Virgin powering for this assembly. The GA 1 and GA 2 resistances improve slightly from assembly 2. This was the final test before moving the sample into the probe for background field performance characterization, discussed later in this report.

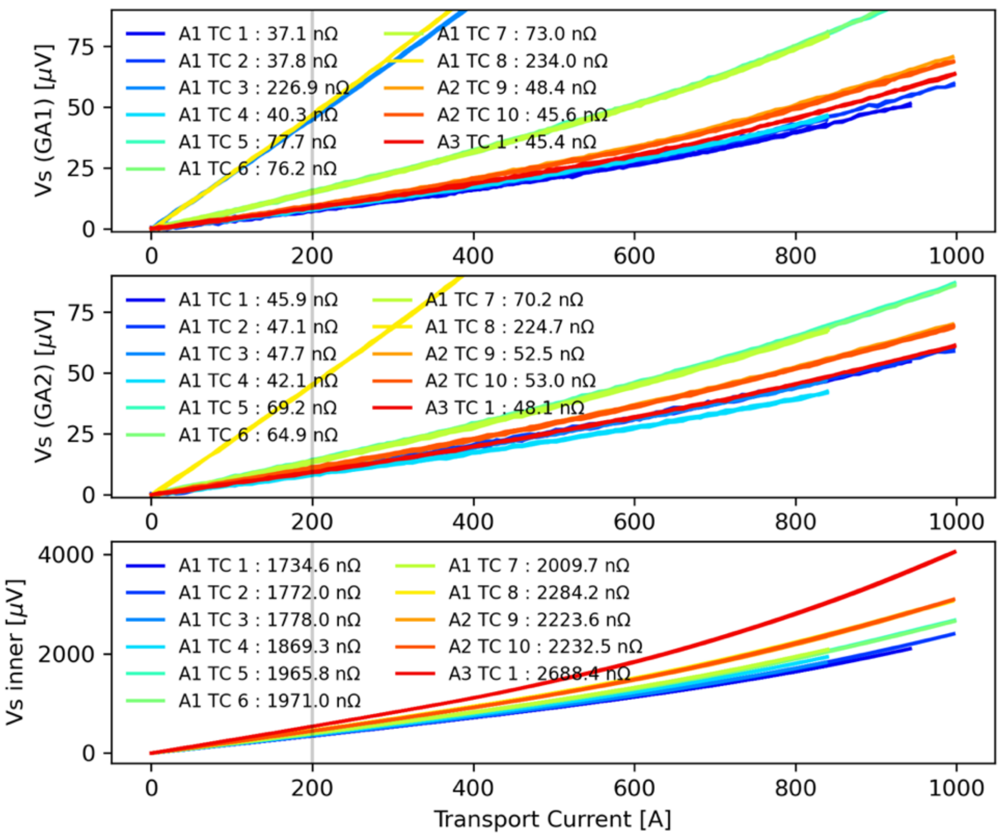

Figure 6: Experimental results of the first assembly (A1) at 77K for eight thermal cycles (TC1-TC8). Some modifications to the sample was done between thermal cycles as described in the text.

As discussed above, a nonlinearity is observed in these I-V measurements of the joint resistance. Figure 6 shows the dame data as Figure 5 however with the 0-200A linear portion removed. This is believed to be an artifact of the upstream joint assembly (i.e. not being able to unfurl tapes with short cable as discussed in Figure 1). One possible explanation is illustrated in Figure 7.

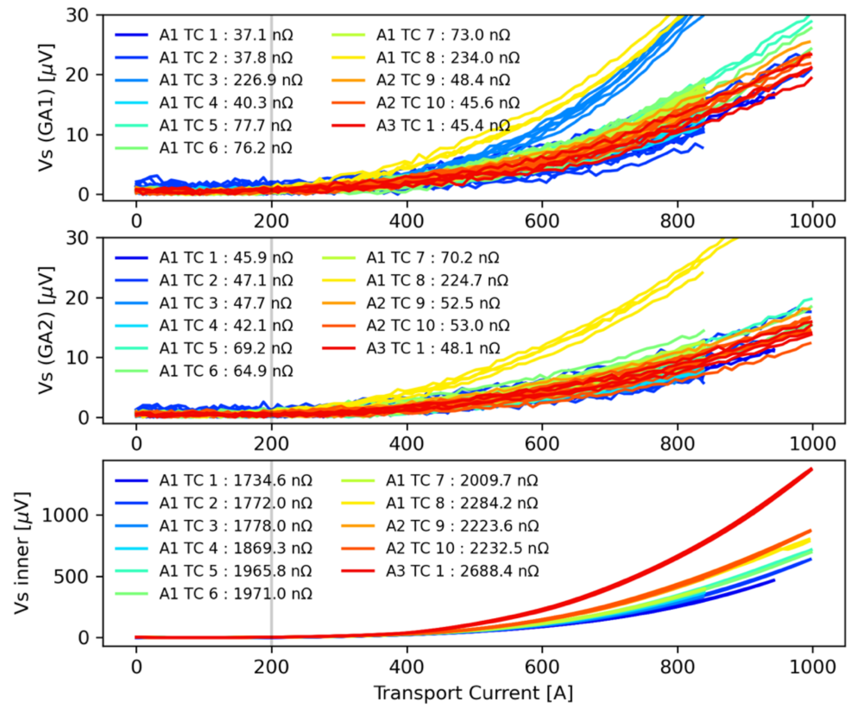

Figure 7: Same data as in Figure 5 above, however with the 0-200A initial linear region removed to highlight the nonlinearity in the joint resistance.

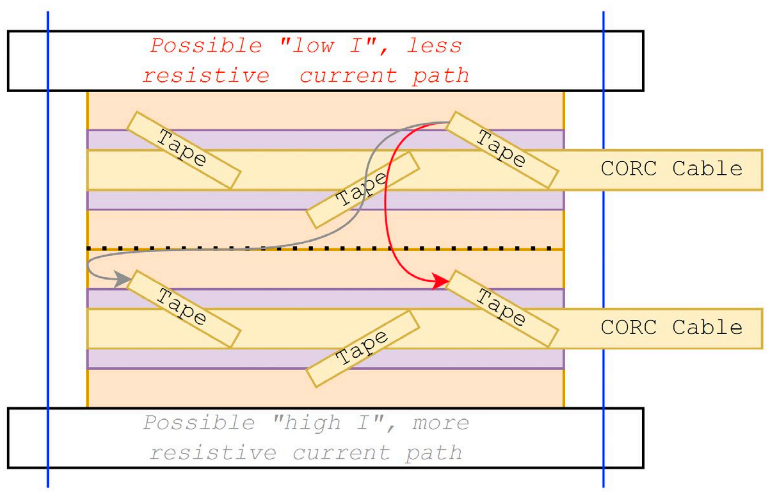

Figure 8: possible explanation for nonlinearity in joint resistance.

2.1 PCB Hall Probe Array

Inspired by ongoing work as in Ref. [2], a PCB Hall probe array was made for the demountable joint sample in this work in an effort to provide insight into the current distribution in the joint. Eight sensors are used as shown in Figure 8; four on the left (A) and four on the right (B). The sensors are located at 25 mm (A1, B1), 75mm (A3, B3), 125mm (A5, B5) and 175 mm (A7, B7) where 0mm is the cable inlet at the left edge of Figure 8. The single axis Hall sensors are oriented along the arrows shown in the left of Figure 8.

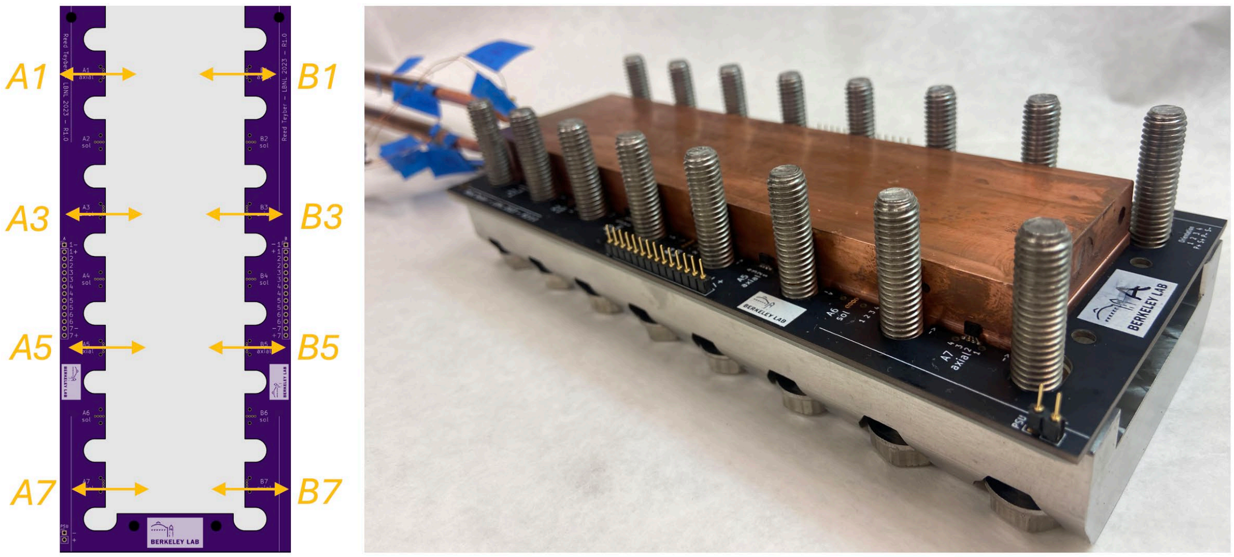

Figure 9: PCB Hall probe array motivated by Ref. [2]

3.0 Bolt Force and Contact Pressure Investigation

This section presents results towards understanding the contact pressure distribution in the demountable joint samples. In addition, the tests above (A1 Thermal 3) highlighted the need to add Belleville washers to maintain clamping pressure in the background field performance characterization. A setup was made to measure the clamping force as a function of tightening torque as shown in Figure 9 below. An Omega LC8200-500-10K load cell was purchased and measured with a Keithley 2010 voltmeter.

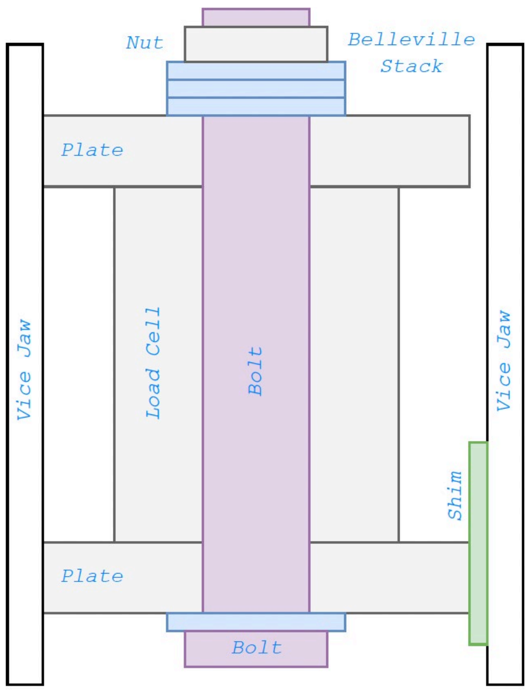

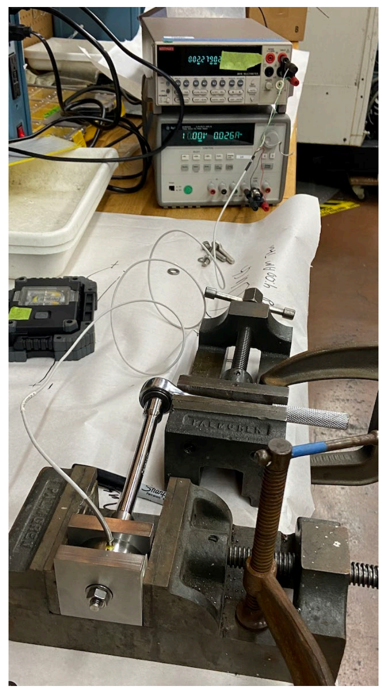

Figure 10: setup with new load cell for measuring bolt force vs. tightening torque for designing Belleville washer stacks.

Inconel 718 Belleville washers were purchased (STS WBEL037F80718) and used with Bumax 109 M8 bolts. The green curve in Figure 10 shows the benchmark case with no Belleville washers and no lubricant, which is how the majority of the LN2 tests were performed above in Figure 5. The black curve shows the addition of three series-stacked STS Inconel washers. For a given applied torque, there was a small reduction in clamping force. The red curve shows the use of white lithium grease. Although this resulted in the highest clamping force, the behavior in liquid nitrogen added an unknown, and we chose to use the dry stack of three Belleville washers (black curve) for the background field characterization. At room temperature and 25 ft-lb of torque, each of the 16 bolts would have around 4,000 lbf.

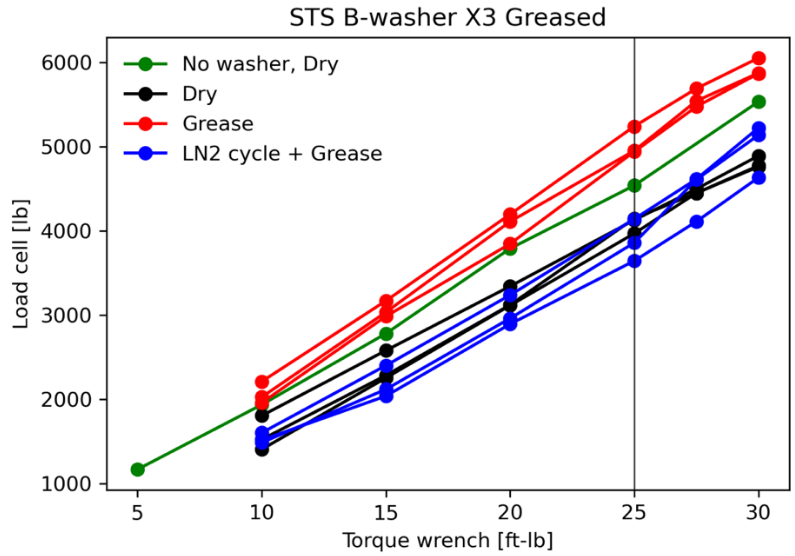

Figure 11: Force-torque measurements on the joint bolts.

Fuji films were then used (50 MPa) to investigate the interface clamping pressure distribution at three bolt torque values (20, 25 and 30 ft-lb). The pressure sensitive films and the supplied reference color chart were scanned and the Cb color from a YCrCb color scale was used to create an interpolant lookup table of color value to pressure as shown in Figure 11.

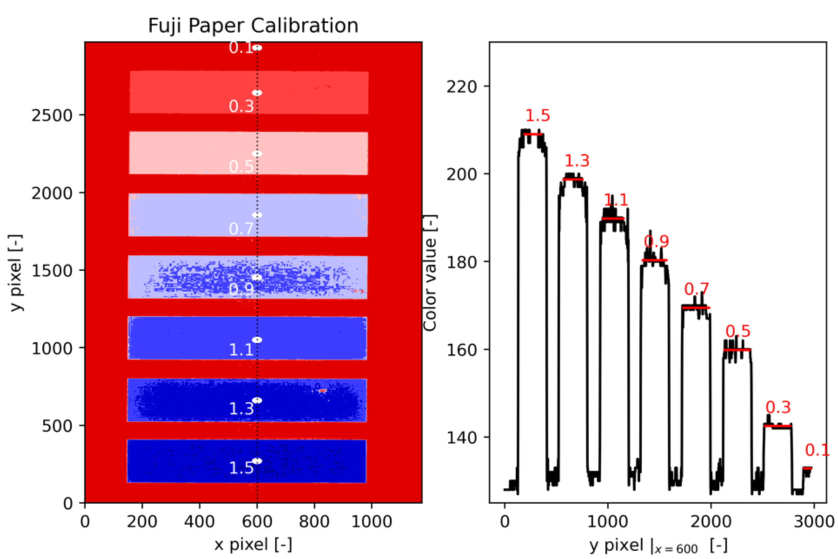

Figure 12: Digitized color reference chart for Fuji films. Right plot shows Cb color value along the vertical dotted cut in left photo, allowing a interpolant lookup table of Cb color value to Fuji film pressure.

Fuji films were clamped in the demountable joint and then scanned, and the resulting color matrices were processed in Python. The processed Fuji films are shown below in Figure 12, showing contours of contact pressure (0-80 MPa) with 20, 25 and 30 ft-lb of bolt tightening torque. The black lines show the 50 MPa contour, showing that the majority of contact pressure is localized along the edges of the interface. Note that the ReBCO tapes are terminated in the center, where the contact pressure is lowest and electrical joint resistance is highest. Understanding and modeling the implications of this on the joint current distribution and performance are a highly recommended area of future research. The 50 MPa contours from the three bolt tightening torques in Figure 12 are shown on a single plot below in Figure 13.

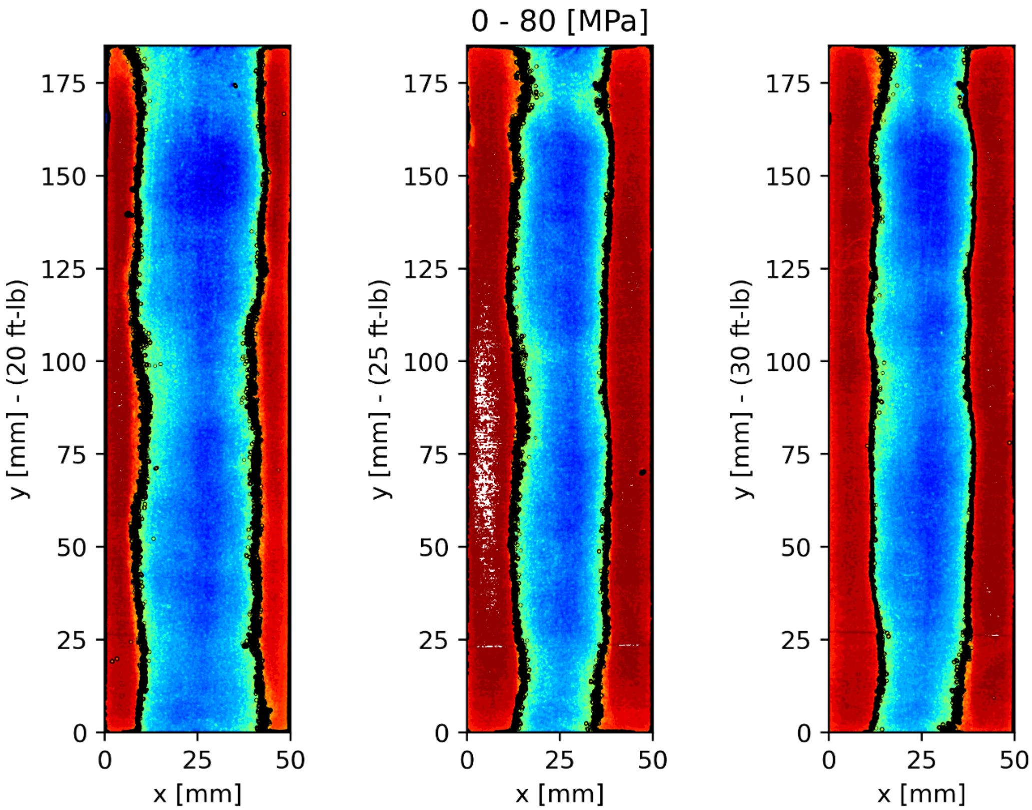

Figure 13: Digitized Fuji films of contact pressure distribution in demountable joint interface using the results of Figure 11.

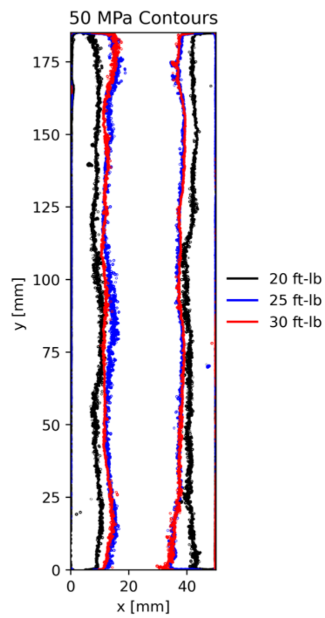

Figure 14: 50 MPa contours from digitized fuji films for three different bolt tightening torques.

It was thought that the joint performance might be improved by increasing or localizing the contact pressure near the superconducting tapes in the center of the joint. A COMSOL mechanical model was created, and a shim of variable width was investigated as shown in Figure 14. Each bolt in the model has 4,000 lbf applied (see Figure 10 above) and the copper and stainless steel properties shown in Table 1. Future work could consider local yielding of the copper at the edges. The simulation results are summarized in Figure 15 for no shim (top), 1.5”, 1” and 0.5” (bottom) shims, showing concentration of the contact pressure near the ReBCO tapes. The color scale shows the contact pressure in units of Pa.

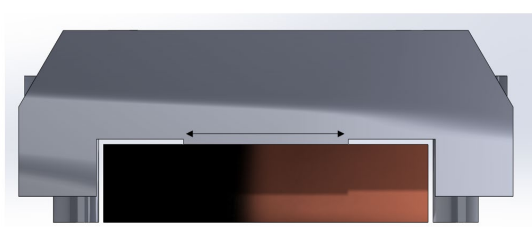

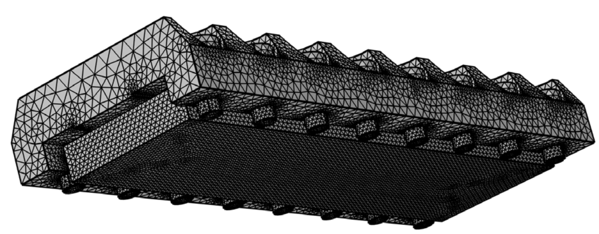

Figure 15: simulated shim (arrows on left) and meshed model for simulating contact pressure in COMSOL

Table 1: Linear material properties used in mechanical simulation

	E [GPa]	ν[-]
Copper	110	0.35
Stainless Steel	200	0.3

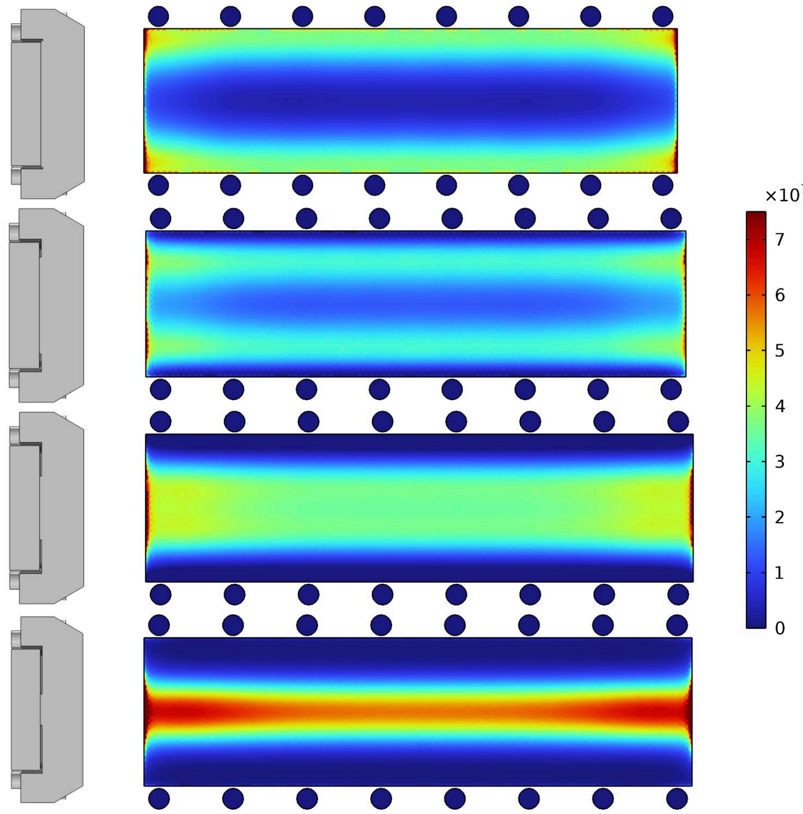

Figure 16: Contact pressure distribution with no shim (top), 1.5”, 1” and 0.5” (bottom) shim. No cylindrical hole for joint was considered in these simulations. Color scale shows units in Pa.

Although not shown here, subsequent simulations with a cylindrical hole for the cable showed that the reduced stiffness presents a practical limit to the level of pressure localization that can be achieved. As such, the 1” shim in Figure 16 was chosen as a compromise between localized pressure near the cable and a relatively high uniformity of clamping pressure across the interface. The digitized Fuji films with the 1” shim are shown in Figure 17, showing the concentrated clamping pressure near the ReBCO tapes. The contact pressure drops off as a result of this reduced stiffness right at the cylindrical hole for the cable.

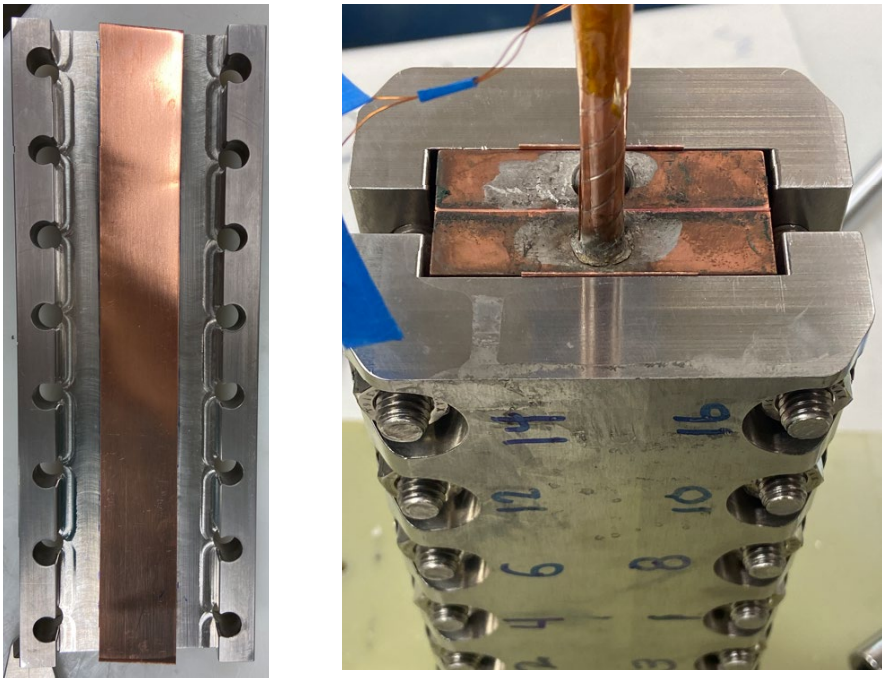

Figure 17: Implementation of 1” shim for concentrating contact pressure in demountable joint interface.

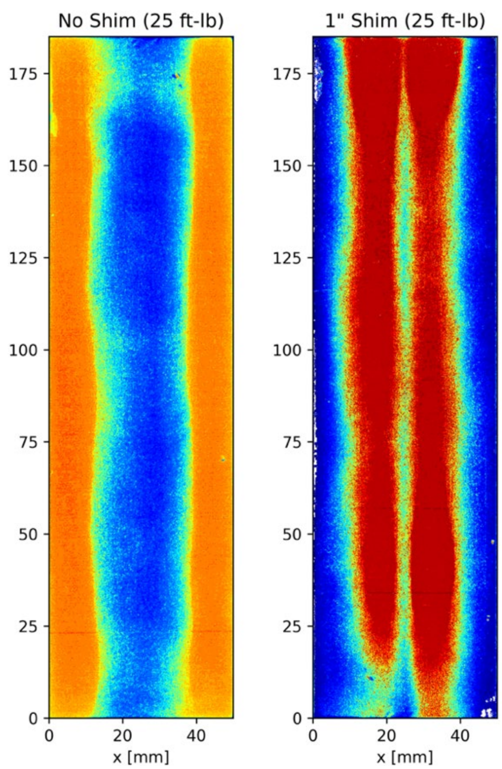

Figure 18: Digitized Fuji films without (left) and with 1” shim (right) with same 0-80 MPa color scale.

The 77 K joint performance with (left) and without (right) the pressure concentrating shim is shown in Figure 18. The top plot shows the I-V characterization, and the joint resistance is shown in legend. Surprisingly, the shim increased the joint resistance from 45 nOhm to 57 nOhm. The dotted line in the top plots show the same I-V measurement as the solid line, however with the initial linear portion removed to highlight nonlinearity in the joint resistance beginning around 600 A. Furthermore, in the case of the 1” shim (left), the two voltage tap resistances GA1 and GA2 are initially similar but diverge around 600 A. The middle and bottom plots show the Hall sensor array measurements (see Figure 8), where the labels (A1-A7, B1-B7) are as shown in Figure 8 above. The bottom plots show the same data as the middle plot, however with the initial linear portion removed. The Hall sensor measurements can be interpreted as a proxy for the amount of current moving toward or away from the particular sensor. Nonlinearities in the current distribution of the joint arise around 400 A, which immediately precedes the nonlinearity in the joint resistance measurement shown in the top plot in both the shim and no shim cases. Comparing the shim to the no shim case, the A1 sensor (solid blue line) changes direction at high currents. This suggests that the addition of the pressure-concentrating shim may cause current to redistribute towards the “front left” of the joint at high currents, possibly resembling Figure 7.

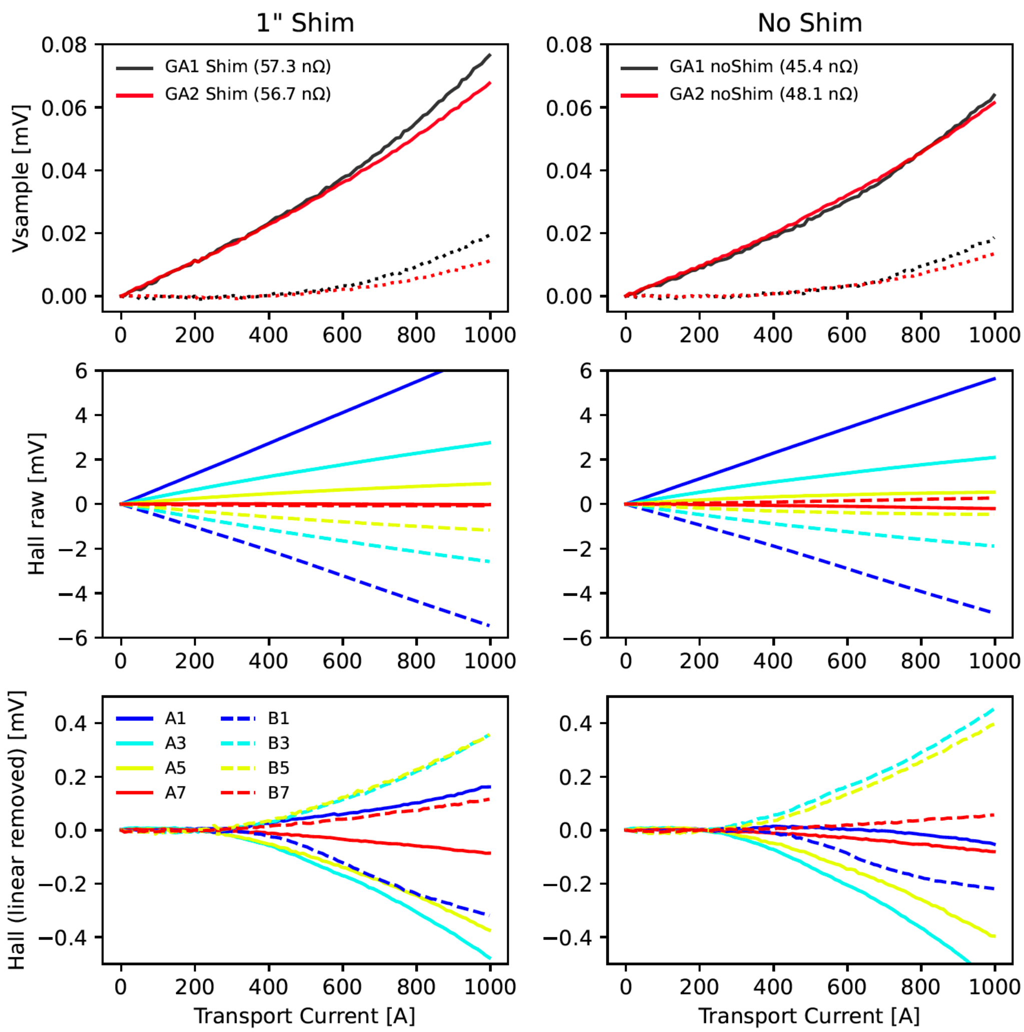

Figure 19: 77 K test results with 1” shim (left) and without 1” shim (right).

4.0 Insert Probe and Facility Preparations

A probe was designed and fabricated to allow joint characterization inside the bore of CCT 5 [3]. The design effort was complicated by the need to support the high joint currents in high background magnetic field, but also to allow full non-destructive disassembly of the assembly after testing. The final design is shown in Figure 19, and the final assembly is shown in Figure 20.

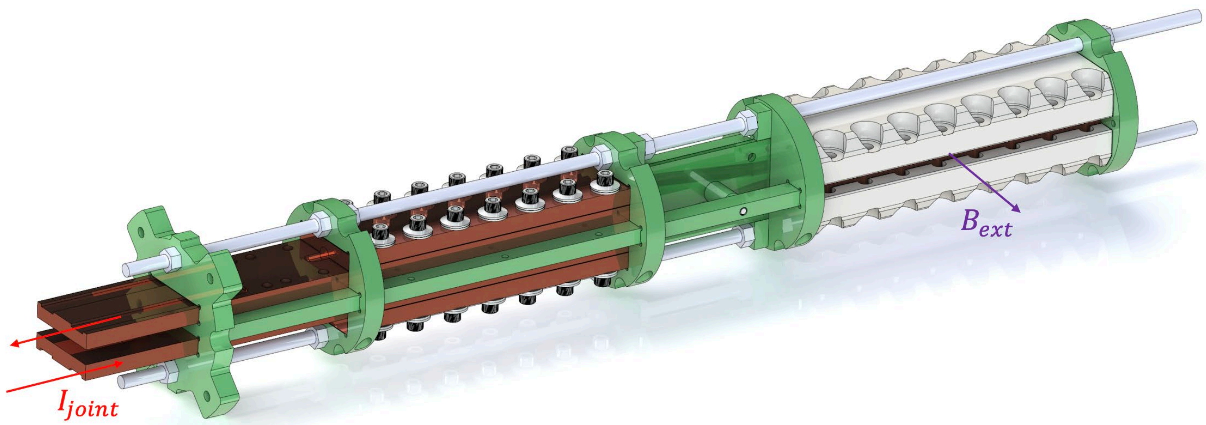

Figure 20: Rendering of joint design, with arrows showing joint powering orientation (red) with respect to the background magnetic field (purple).

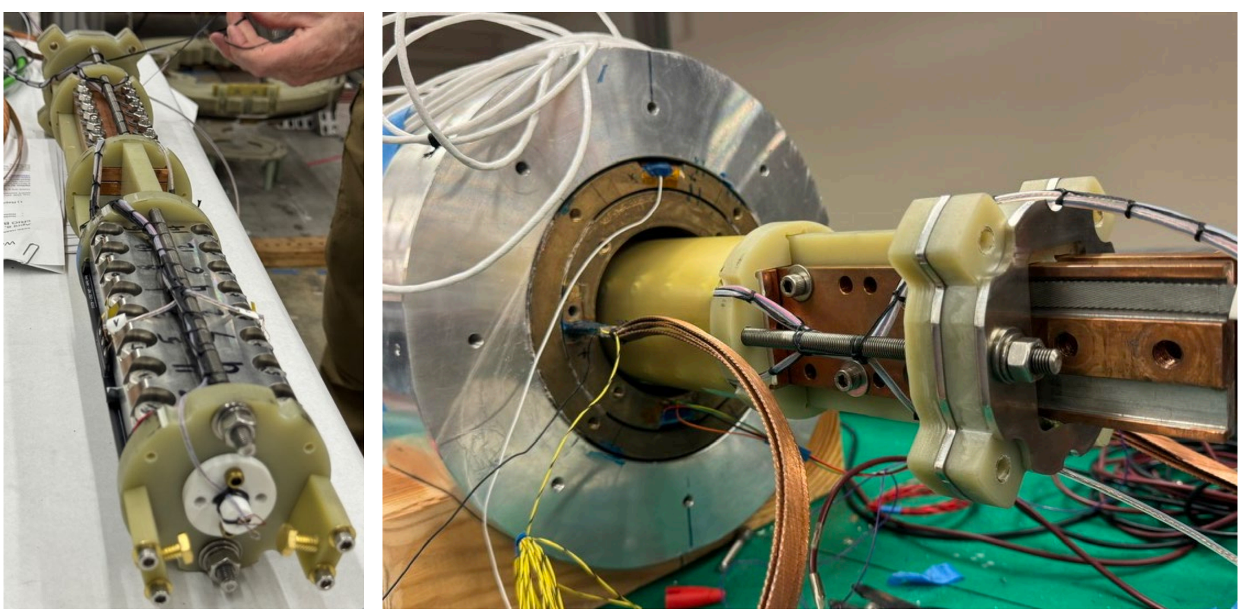

Figure 21: Assembled probe (left) insert in bore of CCT 5 background field magnet (right).

The joint background field performance characterization requires unique and state-of-the-art testing capabilities. The background magnetic field is produced by CCT 5 [3], a 9.7 T (short sample limit) accelerator dipole with a 90 mm bore. Operating this magnet requires the use of the LBNL 25 kA power supply, along with the FPGA quench detection system for triggering IGBT switches to activate a dump resistor for magnet protection. The INFUSE scope here requires a second powering circuit to power the demountable joint (4.8 kA stack of Sorensen power supplies), a second FPGA quench detection system, and a second IGBT-switched dump resistor protection system in case the insert quenches during testing. What complicates the test here is that either the insert (GA joint) or outsert (CCT 5 [3]) may quench during powering, and the two powering and protection circuits need to be coupled with sub-millisecond timing. Furthermore, the cryostat top plate (i.e. header) needs to be modified to accept four vapor cooled leads, with high current bus bars feeding current to the two power circuits. Although the US Magnet Development program, a DOE office of High Energy Physics (HEP) program, funded the majority of the LBNL test facility upgrade to enable hybrid testing of HTS insert dipoles inside of Nb3Sn outsert dipoles, the INFUSE project was used to procure and develop the FPGA system for the insert power supply control, insert quench detection and insert data acquisition shown in Figure 21. These developments enabled our ability to deliver on the INFUSE project scope.

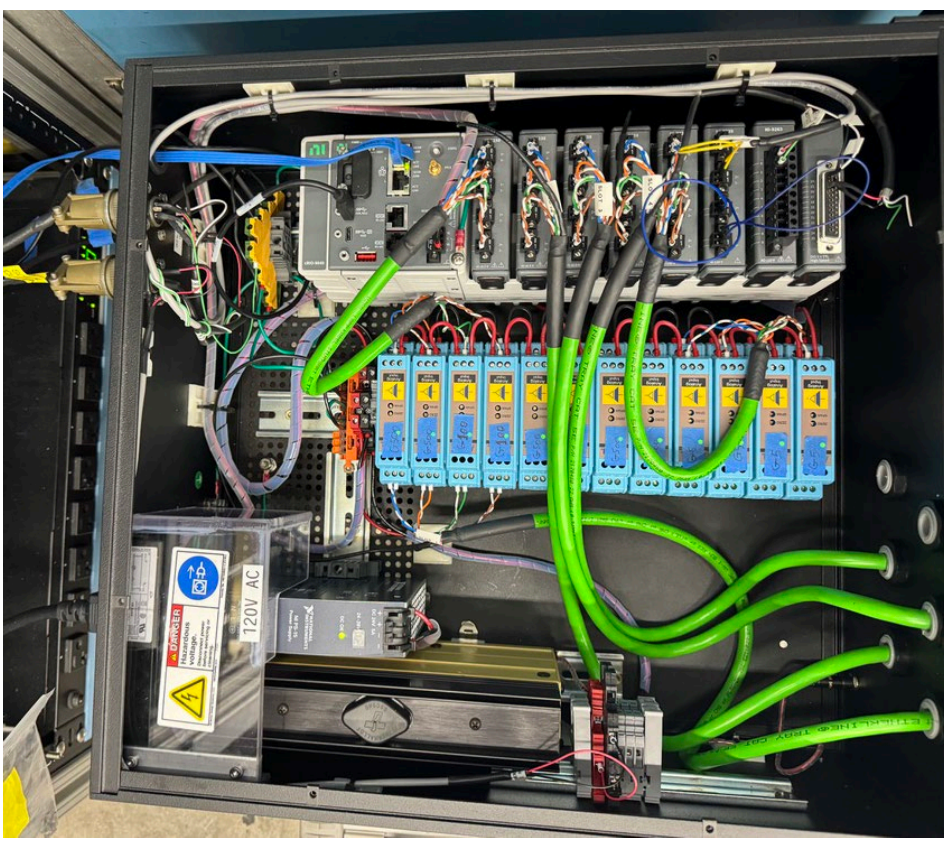

Figure 22: Contribution from the INFUSE project to the LBNL hybrid test facility – the FPGA system and measurement cards for insert power supply control, quench detection and data acquisition.

The assembled probe was tested with this new measurement setup in the final assembly before background field performance characterization. The stairstep ramp is shown Figure 22 at 77 K, and the resistance evaluated between the two points denoted by red circles in the bottom plot show joint resistances of 22 nOhm and 25 nOhn for voltage pairs GA1 and GA2, respectively. This is suspiciously lower than the data in Figure 5. One key difference between the tests was that the perimeter of the interface was coated with Apiezon grease ("cryo-caulk") in an attempt to prevent moisture or air from weeping into the interface, motivated by the corrosion in Figure 3. The grease on the joint interface is shown below in Figure 23. A second difference was the new power supply, control, data acquisition and isolation amplifiers. A current source was used with a resistor to produce a small, known voltage to individually check every measurement channel to confirm the measurement gains - with no surprises. This improved performance at this stage in the program needs further investigation and will be revisited in the discussion section of this report.

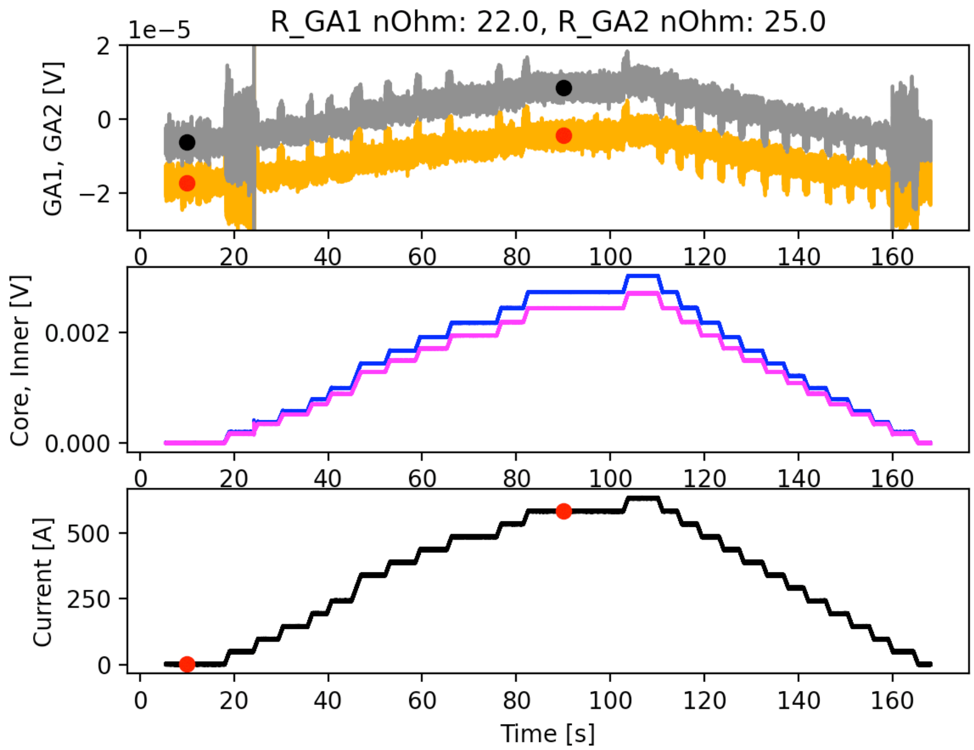

Figure 23: Final 77K performance characterization in new joint assembly

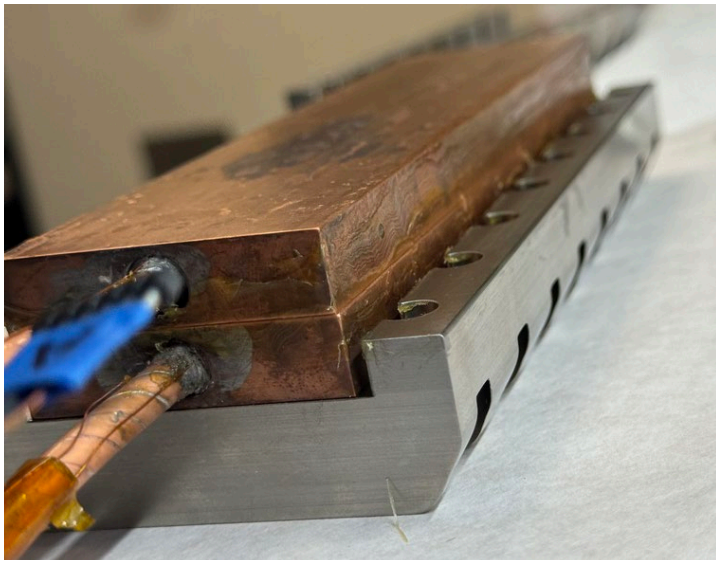

Figure 24: Final assembly of joint before insertion into probe and CCT 5 [3] for background field performance characterization, highlighting interface perimeter grease.

After this final 77K performance test, the joint was inserted into the bore of CCT 5 (see Figure 20 above), and the laborious test preparation commenced. This report will not attempt to cover all aspects related to the preparation of the test, however the INFUSE program funded a considerable design, engineering and technician effort to bring the test to fruition and deliver on the project scope. Figure 24 shows the final assembly on the header while it is being lowered into the test pit. Figure 25 shows the header buildup and facility with the magnet and joint in the pit. 1,500 Liters of liquid helium was purchased and consumed for this test.

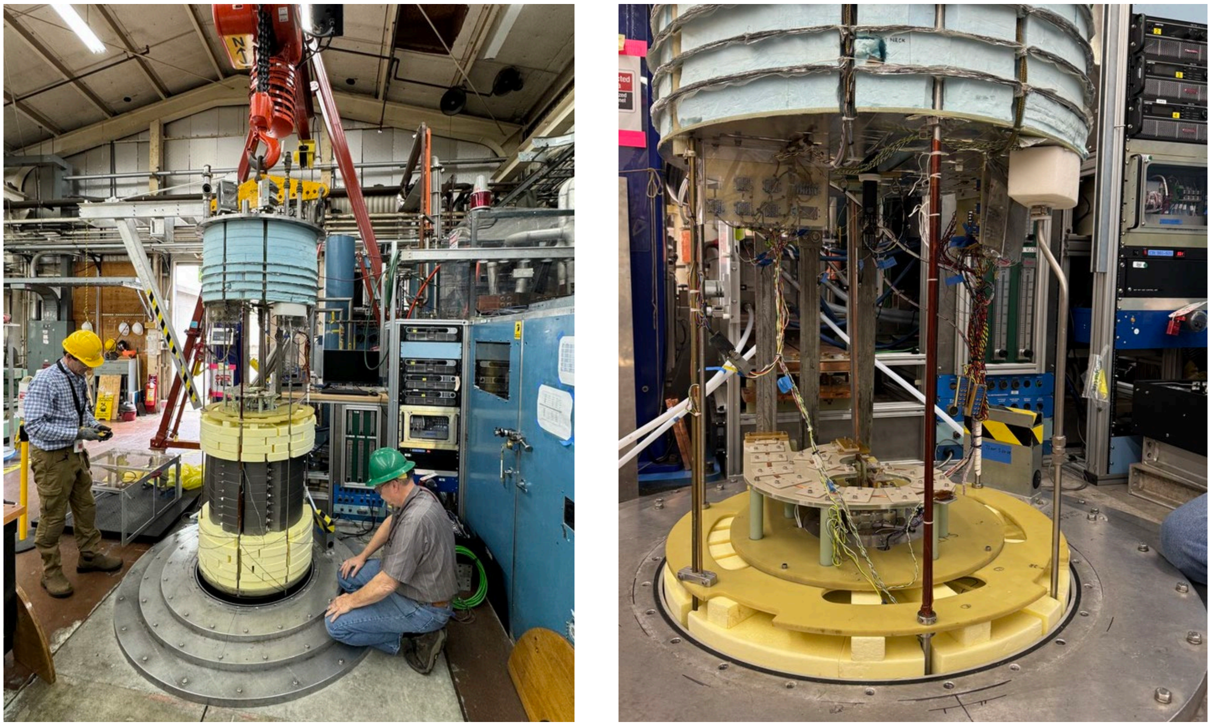

Figure 25: Left photo: Final assembly of CCT 5 (yoke and yellow displacement foam seen) and GA joint on header being lowered into testing pit by Chet Spencer (yellow helmet) and Jim Swanson (green helmet). Right photo: highlighting the wiring harnesses and hardware for routing the four high current leads to the four vapor cooled leads.

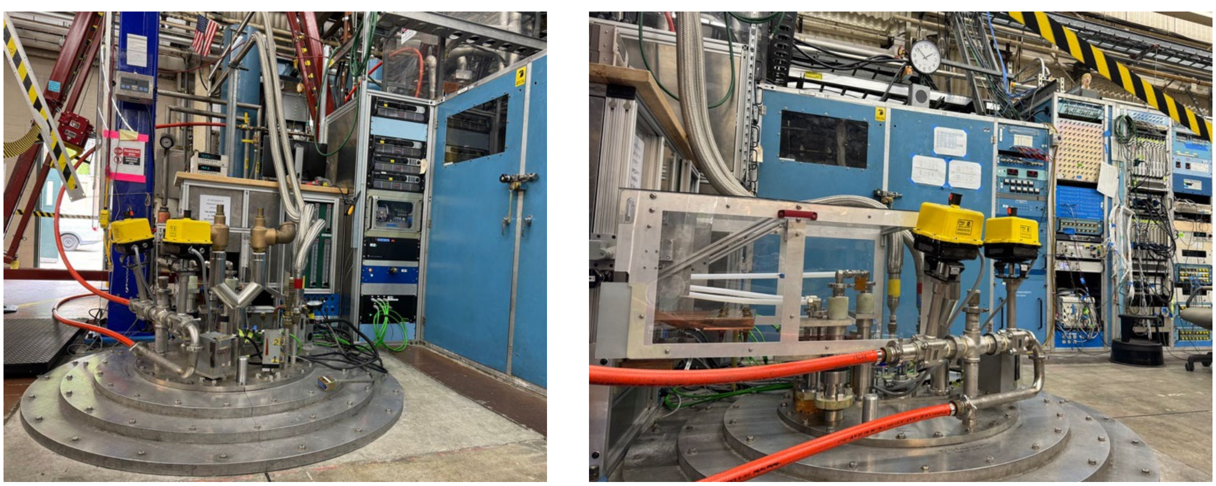

Figure 26: Header buildup and test facility preparation with CCT 5 and GA demountable joint in pit.

5.0 Background Field Performance Characterization of CORC Demountable Joints

The joint I-V measurements as a function of background magnetic field are shown below in Figure 26. For these measurements, the background magnetic field is first ramped up to the value shown in the legend, and then the joint is powered to 2.4 kA in a trapezoidal waveform with constant background magnetic field. The plot below contains both an up and down ramp, and the constant inductive offset is seen. The similarity in slope and shape between the up and down ramps give confidence on the measurement and protocol. These measurements are filtered, and a very good signal-to-noise is obtained even with the isolation amplifiers that are required for these types of tests. A piecewise-linear kink is observed around 1200 A which becomes more pronounced with elevated field. High voltages during IGBT switching of the background field dump resistor system limited the joint background fields to 6 T in this program.

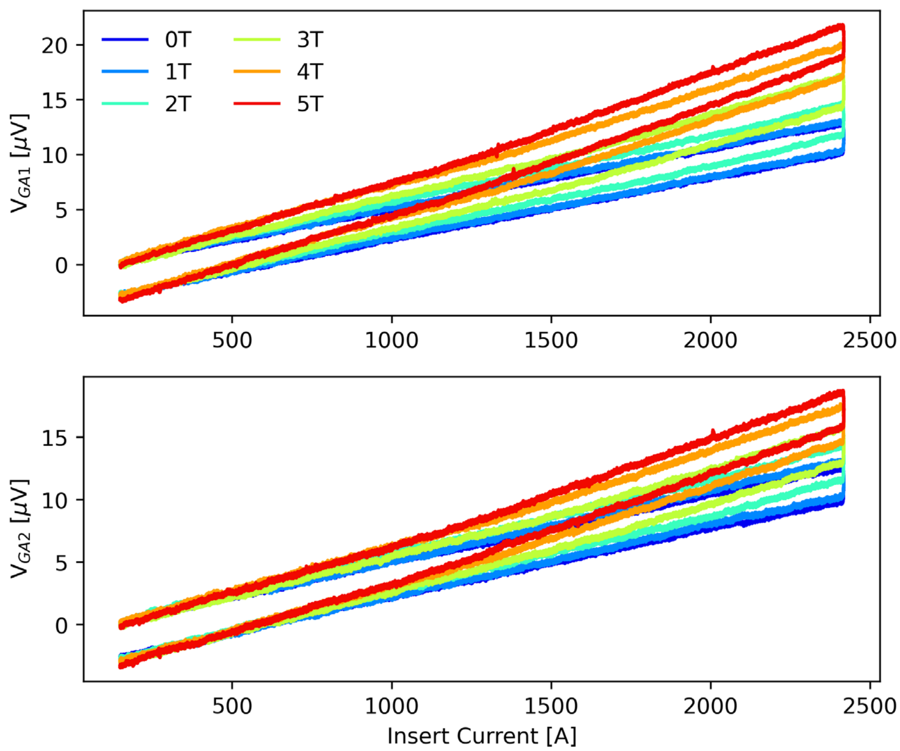

Figure 27: V-I measurements of demountable joint sample as a function of background field. Top plot is voltage tap GA1 and bottom plot is voltage tap GA2.

The resistance as a function of background magnetic field, evaluated at the 0 A and 2.4 kA (at the dwell) points, is shown below in Figure 27. The top plot shows GA1 and the bottom plot shows GA2. The first set up measurements was performed in increments of 2 T up to 6 T on June 3/5. The second set of measurements was performed on June 6 in increments of 1 T up to 5 T. For both GA1 and GA2, the initial joint resistance is ~ 5-6 nOhm, increases nonlinearly around 2 T, and increases almost linearly to ~10 nOhm at 6 T.

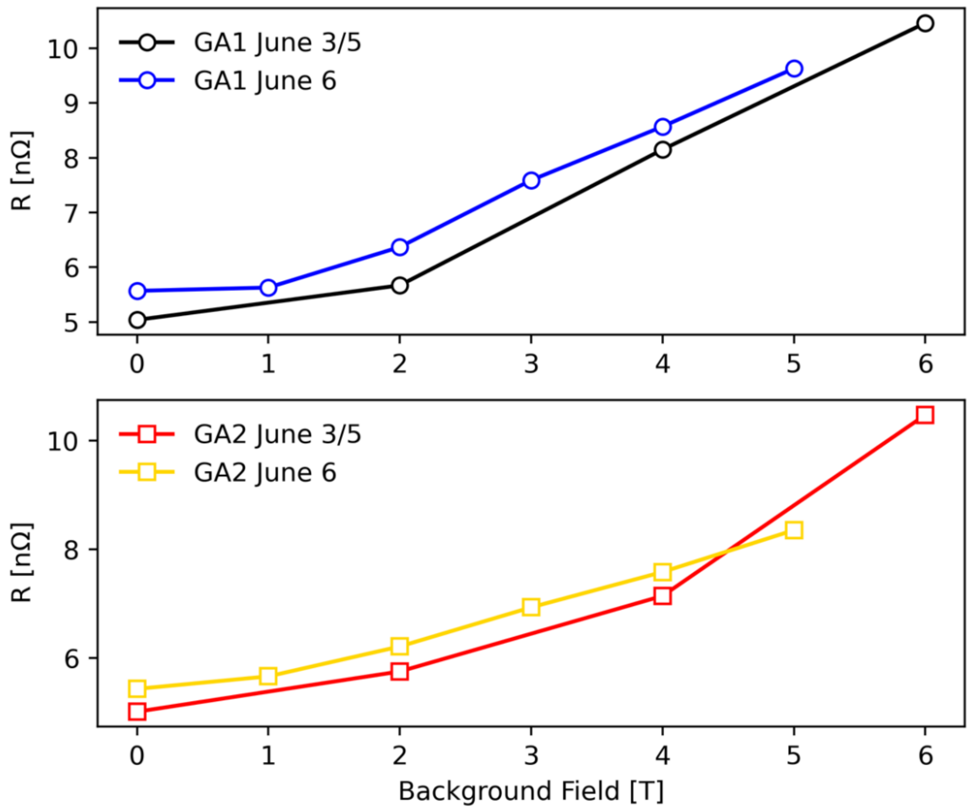

Figure 28: Joint resistance as function of background magnetic field

A separate test protocol is now presented as shown below in Figure 28. Here, the insert current is first ramped to 2.4 kA followed by a ramp of the outsert current, providing a continuous resistance as a function of field curve. The results are shown in Figure 29, where the bold curve shows a low pass filter applied. The circle at B = 0 T shows the resistance evaluated at the two points of the vertical dotted blue lines in Figure 28. Similar to the other measurement protocol in Figure 27, the shape of the R(B) curve is initially flat, then rapidly increases around 0-2 T, and then is more linear with a slightly decreasing slope. Although the joint resistance as measured by GA 2 is similar for the two test protocols, the continuous background field ramp resulted in a significantly elevated GA 1 joint resistance nearing 13 nOhm at 5 T. This is not fully understood, however the inductive voltages from the ramped background field may alter the cable current distribution such that current is forced to flow through tapes with elevated termination resistances. This could be an impactful topic for future modeling and investigation.

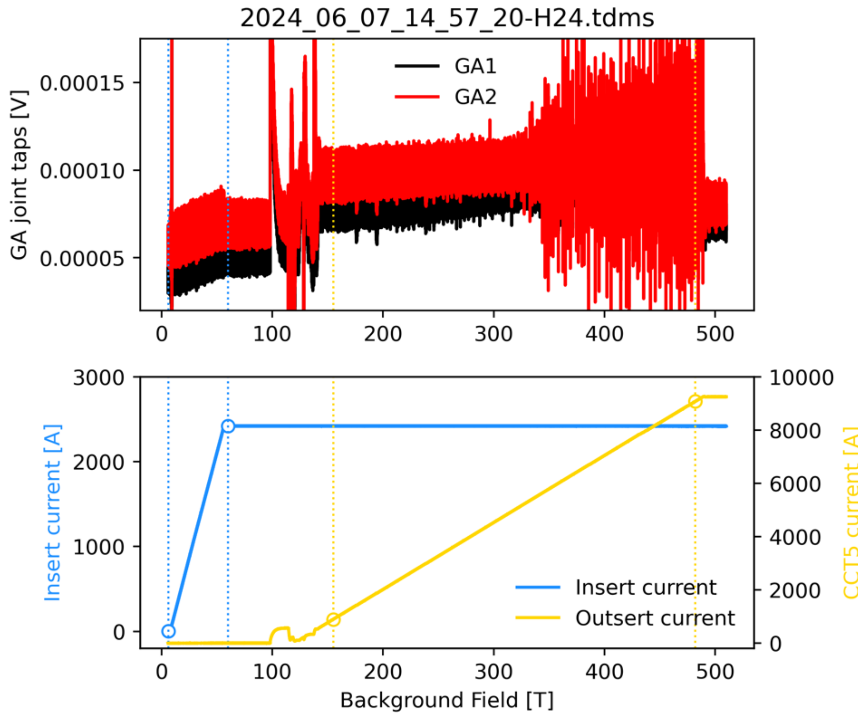

Figure 29: Powering protocol and measurement results for continuous R(B) measurement.

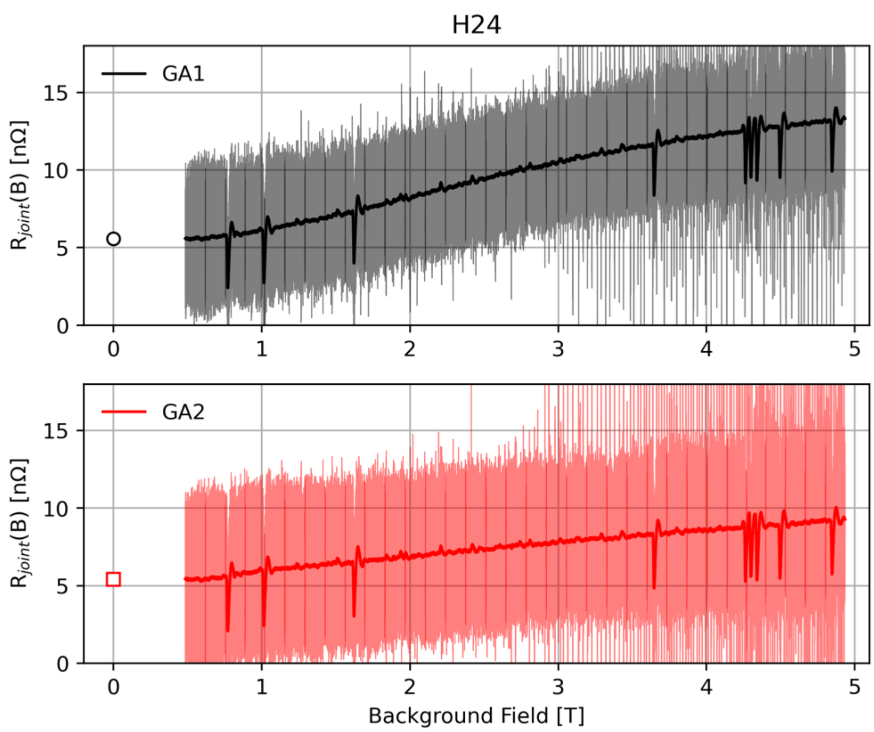

Figure 30: Continuous R(B) measurement obtained from ramping background field with constant joint current

The magnetoresistance of copper is quite linear, and hence it would be expected that the R(B) curve would follow this linear trend. One possibility behind the R(B) curve shape is described here. Figure 30 below shows the simulated field distribution of the background field magnet superimposed over the geometry of the demountable joint samples shown to scale. The short CORC cable lengths protruding from the joint (see discussion around Figure 1) result in a relatively large field gradient across the upstream joints. Considering the 5 T case, the outermost layer is terminated at the left end (~x=200 mm) in a field above 3 T, and the innermost layer is terminated at the right end (~x=400 mm) in a field around 0.5 T.

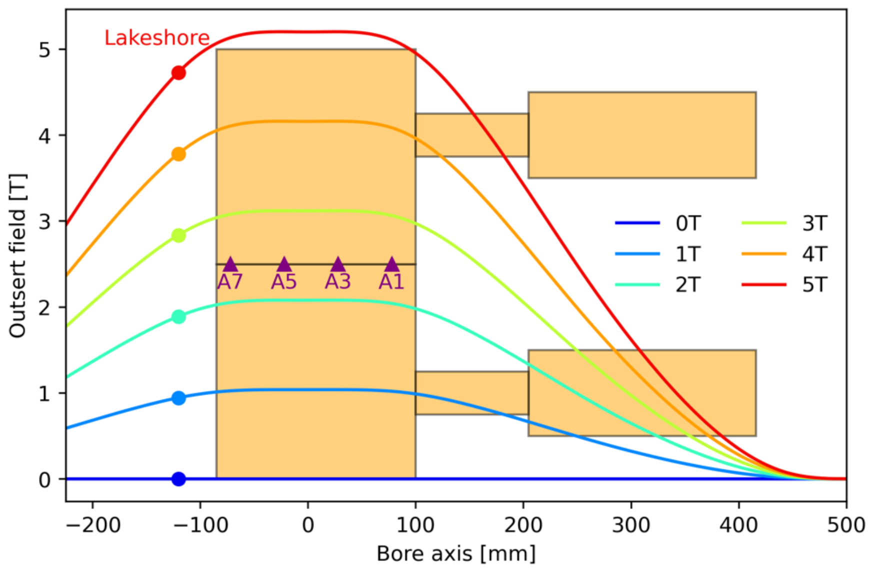

Figure 31: Field profile from background field magnet. Note that the front of the upstream terminations (right rectangles) is exposed to a field gradient.

The PCB Hall array measurements are shown in Figure 31, where the joint illustration and sensor labels are consistent with Figure 30 above. All the measurements are normalized to the B1 sensor. As the background field increases, the curves at the left side (~x=-75mm) shift upwards, and these curves shift up most rapidly in the 1-2 T range. This 1-2 T range coincides with the onset of R(B) nonlinearity in Figure 29. The increasing magnetic field along the left side of the plots signal that more current is flowing in the rear of the joint, which suggests that more current is flowing in the inner-most layers of the CORC cable (see Figure 1 showing tapered layers). Figure 30 above shows the field gradient places the outer layer termination in a higher magnetic field than the inner layer termination.

This hypothesis is further supported by the previous V-I data in Figure 26 above. A bi-linear trend is observed (i.e. “kink”) in each V-I plot, and the kink is more pronounced as the magnetic field increases. The 0-2 T curves in Figure 26 are almost fully linear; around 3 T, a kink initiates around 1,200 A joint current and becomes most pronounced with 5 T background field. This is not referring to the overall change in slope with field, but to the presence of the bi-linear behavior that originates around the vicinity of the current redistribution phenomena measured with the PCB Hall probe array in Figure 31 and discussed in the previous paragraph. This points – as one possibility – to elevated termination resistances in a subset of tapes in the cable that increases with background field, i.e. non-uniform tape termination resistances driven by the termination field gradient shown in Figure 30.

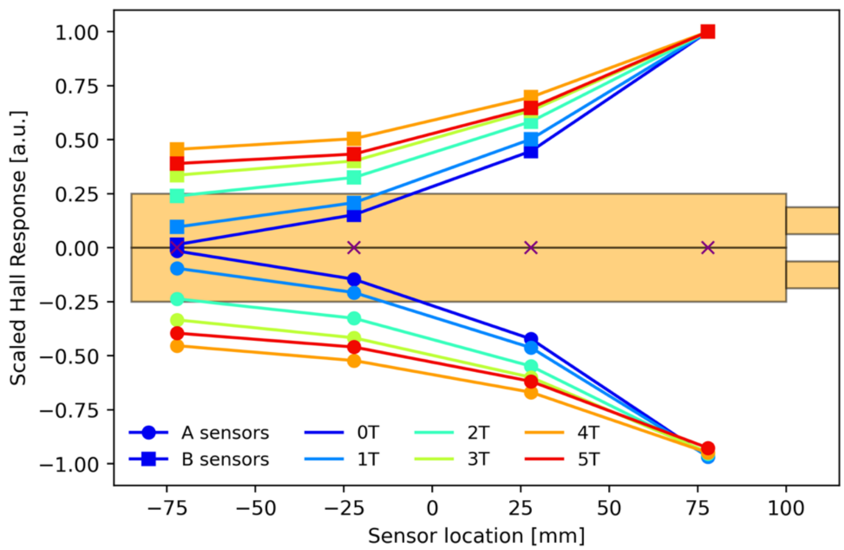

Figure 32: Hall sensor array measurements during background magnetic field.

6.0 Unresolved and Driving Questions

The characterization of joint resistance as a function of background field – the key deliverable in the INFUSE program - completed the remaining project funds. The following list outlines questions which arose during the program, and would be excellent topics for future research towards enabling demountable HTS fusion magnets.

- What is the RRR of the joint sample tested here?
- What is the mechanism of the corrosion found on the samples, how can it be avoided, and what is the impact on the joint resistance?
- Why did the 77 K joint performance improve in the final assembly before the background field characterization? What is the 77K resistance of the sample in this report after the background field characterization?
- Why did the R(B) curves differ between the two test protocols? If it is the inductive voltage driving a sub-optimal current distribution in the cable, do we understand this well enough to recreate the physics via a predictive model?
- What is the interface resistivity, and what is the impact of the contact pressure on interface resistivity? What is the resulting impact of the contact pressure distribution on the current distribution and overall joint performance?
- What are the individual tape terminations resistances in the joint samples? What is the difference in resistance between different tape combinations? (e.g. inner layer cable A – inner layer cable B, inner layer cable A – outer layer cable B, …)
- What are the contributions of each component (tape solder, bulk copper, interface) to the resistances measured during this program? What are the practical lower limits of each resistance component (tape solder, bulk copper, interface), what are the sensitivities of resistances to design variables and process parameters, and how do we produce demountable HTS joints nearing these performance limits?

4.0 Conclusion

The DOE FES INFUSE program between GA and LBNL is reported, starting with the initial sample preparation and 77K performance characterization results. These initial results motivate an effort to measure, simulate, and manipulate the interface contact pressure distribution with varied levels of success. PCB Hall probe arrays are developed and implemented to better understand trends in the joint operation and current distributions. Although funded by a different program (DOE office of High Energy Physics), the first phase of the LBNL hybrid test facility upgrade is completed with an important contribution from the INFUSE program detailed; the FPGA system for the insert (joint) power supply control, quench detection and data acquisition. The completion of the facility upgrade enables the dual magnet powering and coupled protection circuits required for the program scope. A bespoke insert probe is then designed and fabricated, and the resistance of the demountable CORC joint as a function of background magnetic field up to 6 T is measured and presented. Joint resistances are on the order of 5 nOhm with no background field and on the order of 10 nOhm at 6 T, which is higher than anticipated. Two test protocols were employed, with slightly elevated joint resistances observed during continuous ramping of the background field. PCB Hall array data suggests that current redistribution to inner cable layers via large field gradients across the upstream cable joint may drive some of the nonlinearity in the joint resistance vs. background field curves, however further analysis and modeling is suggested. The need for high voltage isolation amplifiers during the background field characterization posed a significant risk to our ability to deliver on our scope, however the resulting signal integrity and measurement quality exceeded our expectations. A list of pressing R&D topics is identified which should be investigated in future research programs, which would play an important role in enabling fully demountable superconducting magnets that allow for fusion machine maintenance.

References

[1] Weiss *et al. "Performance of Low-Loss Demountable Joints between CORC Cable-In-Conduit-Conductors at Magnetic Fields up to 8 T Developed for Fusion Magnets"* (2023), Supercond. Sci. Technol. 36 085002.

[2] Teyber *et al. "CORC cable terminations with integrated Hall arrays for quench detection"* (2020), Supercond. Sci. Technol. 33 095009

[3] D. Arbelaez *et al*., "Status of the Nb3Sn Canted-Cosine-Theta Dipole Magnet Program at Lawrence Berkeley National Laboratory" (2022), IEEE Trans. App. Supercond. 32 (6) 4003207